Chapter 7

Study of Pt growth on oxygen-covered Ni(110) surfaces

7.1 Introduction

This chapter focusses on an attempt to grow thin Pt films on a metallic substrate, as such films would provide more cost-efficient surfaces for catalytic processes. Instead of using a large Pt crystal, a thin film could be deposited on a cheaper metal substrate and still provide the properties necessary for a given catalytic process, such as in the production of nitric acid via the oxidation of NH_3 molecules [129].

The study of thin Pt films deposited on a clean Ni surface has mainly concentrated on the (100) and (111) faces. Using AES, RBS and LEED, Deckers *et al*. [186] found that room temperature Pt deposition led to the formation of a disordered Pt thin film on top of the Ni(111) substrate. Growth at 250 °C, however, led to the growth of a pseudomorphic Pt film. Both growth at 350 °C and annealing samples at 450 °C led to the formation of an alloy with an overall Ni:Pt ratio of approximately 1:1. Using RBS, the alloy was observed to have an abrupt interface with the Ni(111) bulk structure. Similar results have been obtained by several different groups and are summarized by Robach *et al*. [187]. In the Ni(100) case, Deckers [188] found that room temperature Pt deposition also led to the formation of a disordered Pt film. Again, alloy formation was observed for both deposition and annealing at 350 °C and above.

In contrast, recent observations by Kellogg using field-ion microscopy [189] have indicated that the adsorption of Pt atoms on the Ni(110) surface leads to the formation of an alloy structure in the near-surface region. However, if the chemical and structural properties of the surface are altered prior to Pt deposition (e.g. by oxidation of the Ni(110) surface), it may be possible to grow thin Pt films on top of the surface. The key objective of the work presented here is to determine the extent to which the

Ni(110) surface must be exposed to atomic oxygen in order to prevent Ni-Pt alloy formation during the deposition of Pt on to an O-covered Ni(110) surface.

The oxidation of the Ni(110) surface has been studied using many different techniques (references [190–194] cover just a few examples). Short exposures to molecular oxygen yield several possible reconstructions at sub-monolayer coverages. Firstly, the (3×1)-O *added row* structure is formed, with O atoms occupying every third row in the <100> direction, as shown in figure 7.1. This corresponds to an O coverage of 0.33 ML. The structure of the Ni(110)-(3×1)-O surface has been studied by van der Veen *et al.* using medium energy ion scattering [195]. This technique is more sensitive than CAICISS in terms of its sensitivity to relaxations in the surface region [1], with an expansion found in the outermost interlayer spacing of $\sim 1\%$ relative to the bulk interlayer spacing following the adsorption of $1/3$ ML of O in order to form the Ni(110)-(3×1)-O surface.

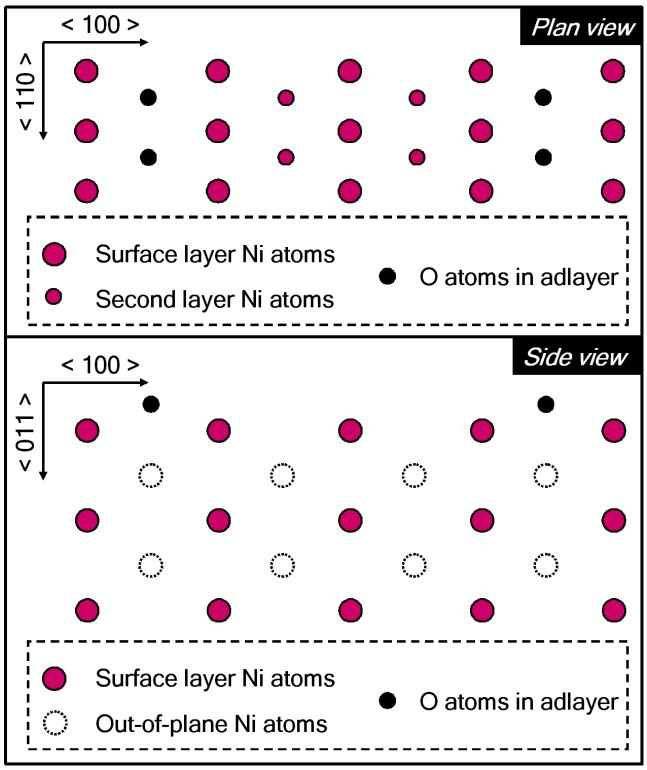

Figure 7.1: A schematic illustration of the (3×1)-O added row structure formed along rows in the <100> direction on the Ni(110) surface. Both the top and side views of the structure are shown.

Increasing the coverage to 0.50 ML results in the formation of a (2×1)-O overlayer, with O atoms in every second row in the <100> direction. At an O coverage of 0.67 ML, the (3×1)-O *missing row* structure is formed, with two out of every three rows in the <100> direction occupied by O atoms. Increasing the O coverage further results in the formation of a *'sub-oxide'* (9×5)-O structure at a coverage of a few ML, before a NiO(110) structure is formed at higher coverages [190]. However, attempts to grow thin films on top of these structures have been very rare.

Previous work on the characteristics of systems involving Pt deposition and O adsorption on Ni surfaces has been largely limited to attempts to oxidise the Ni substrate following Pt deposition [186, 188, 196]. In general, this work has shown that a small coverage of Pt acts as a barrier to the oxidation of the underlying Ni crystal. This is hardly a surprising result, given the low saturation coverage of O_2 on Pt surfaces described in chapter 5. To date, no investigations of the growth of Pt on the Ni(110)-(3×1)-O or NiO(110) surfaces have been published.

The work detailed in this chapter takes the observation of the formation of a Ni-Pt surface alloy on the Ni(110) surface, reported by Kellogg [189], and attempts to alter the growth mode by exposure of the Ni(110) surface to oxygen, prior to Pt deposition. Firstly, the Ni(110) surface was exposed to a small amount of oxygen in order to form a (3×1)-O overlayer in an added row type structure along the <100> direction, as shown in figure 7.1. Following an investigation of this structure, Pt was deposited on the surface, with the growth mode and layer-by-layer composition determined using CAICISS, LEED and XPS. Then, following cleaning, the Ni(110) surface was heavily oxidised, with CAICISS, XPS and LEED used to characterise the near-surface region. Finally, Pt was deposited on the oxidised Ni surface to observe any possible differences in the growth mode of Pt on the NiO(110) surface, compared to growth on the Ni(110)-(3×1)-O surface.

7.2 Experimental details

The experiments were carried out on the Warwick modular CAICISS system, detailed in chapter 3. The Ni(110) crystal was aligned to an accuracy of 0.1° (verified

by Laue measurements), spark eroded and mechanically polished prior to being loaded into the scattering chamber. Once loaded, the crystal underwent further *in-situ* cleaning via cycles of low energy IBA (3 keV Ar^+ for 30 minutes, followed by annealing at 700°C for 1 hour). The surface was deemed to be clean following the observation of a sharp (1×1) LEED pattern with low background intensity, and negligible concentrations of C, O or other contaminants in the XPS spectrum. All XPS data were recorded using the Mg K_α anode ($h\nu = 1253.6$ eV), with the binding energies calibrated using the Ni $2p_{3/2}$ peak at 852.3 eV [142]. The analyser was operated in fixed analyser transmission (FAT) mode, with a pass energy of 25 eV. Resistive heating of the sample up to 700°C was monitored using a chromel-alumel thermocouple in contact with the sample. All CAICISS data were taken in the <100> direction using a 3 keV He^+ ion beam, with a step time of 100 s and a polar angle rotation of 1.8° between each step.

Atomic oxygen adsorption was carried out in pressures of 10^{-7} to 10^{-8} mbar using the OAR TC-50 thermal gas cracker, which has an estimated cracking efficiency of ∼ 60 % for O_2 [143]. Pt deposition was carried out using a metal evaporation source consisting of a high-purity Pt wire wound around a tungsten filament.

7.2.1 Scattering geometries

All the CAICISS data presented in this chapter were acquired in the <100> azimuth, with the scattering geometries which give rise to each peak being shown schematically in figure 7.2. This azimuth offers the opportunity to probe the structure down to at least the fifth atomic layer, with a chance that the seventh atomic layer is visible close to directions 4 and 5 if the atoms in the either the first or fifth layers focus some ions deeper into the structure. The geometries shown in the figure show scattering in the odd-numbered layers, but it should be noted that a similar set of geometries exist for the even-numbered layers (represented as dashed circles in figure 7.2. Therefore any relaxations in the surface region will manifest themselves as additional features in the CAICISS spectra.

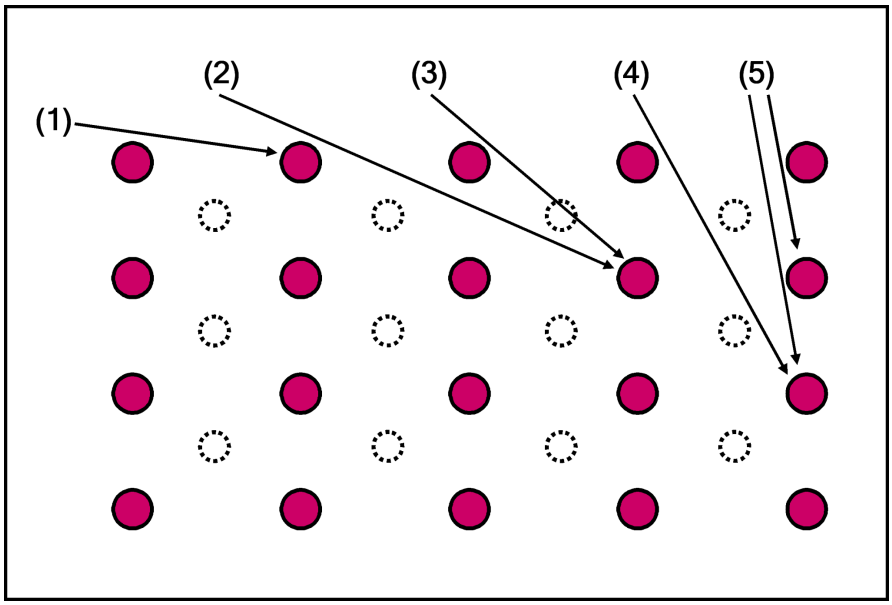

Figure 7.2: The scattering geometries which give rise to peaks in the CAICISS data recorded in the <100> azimuth on an f.c.c. (110) surface. Geometries corresponding to odd-numbered layers are shown here, with atoms in these layers represented by the filled circles. The atoms in the even-numbered layers lie in a different plane and are represented by the dashed circles.

7.3 The Ni(110)-(3×1)-O surface

The first part of the investigation focussed on the changes to the structure of the Ni(110) surface as a result of oxygen adsorption in order to form a (3×1)-O added row overlayer structure. The determination of this structure is necessary in order to distinguish any changes to the structure which may be due to the Pt depositions carried out in the next section of this chapter, information which is crucial to finding differences between Pt deposition on the Ni(110)-(3×1)-O surface and the work carried out by Kellogg on the Ni(110) surface [189].

Studies of the structure of the clean Ni(110) surface have been conducted using various techniques and, in general, have found consistent results. Examples from the literature are given in the reviews by Rodríguez *et al.* [12] and Ting *et al.* [197], which illustrate a pattern of relaxations in the outermost layers of the structure. In general, the outermost interlayer spacing, Δ_{12} has been observed to contract by around 7% to 1.16 Å. The next spacing, Δ_{23}, expands by around 3.5%. Below this, the structure

reverts to the bulk Ni(110) structure, with interlayer spacings of 1.246 Å.

The Ni(110)-(3×1)-O surface was formed by exposing the clean Ni(110) surface to 1.0 L of atomic oxygen, generated using the thermal gas cracker. The LEED patterns observed prior to and following the oxygen exposure are shown in figure 7.3. CAICISS data were then taken in the <100> azimuth, with the Ni-backscattered intensity profile extracted from the data shown in figure 7.4(a). In this profile, the peak at 14° corresponds to scattering from Ni atoms in the surface layer and, using equations 3.13, 3.14 and 3.15 yields an interatomic spacing (and also lattice constant) of 3.52 ± 0.05 Å, a value in line with the known lattice constant of Ni [60].

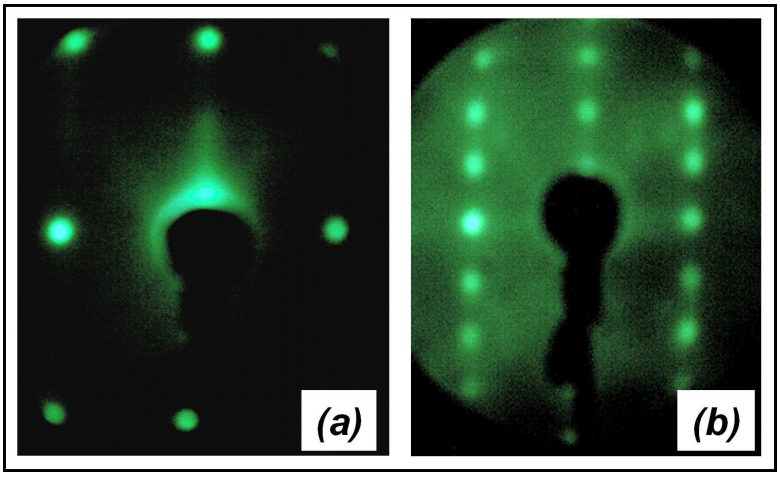

Figure 7.3: LEED patterns observed from (a) the clean Ni(110) surface at 78 eV, and (b) the (3×1) pattern observed at 92 eV following exposure of the clean surface to 1.0 L of atomic oxygen.

Moving to increasing polar angles, the peaks centered at 27°, 46° and 64° correspond to scattering from various individual scattering geometries in the sub-surface region (see figure 7.2), whilst the peak centered at 72° corresponds to scattering from several different layers of the structure. Therefore, fitting of these peaks enables the sub-surface structure to be derived.

Analysis of these data was carried out using the FAN software, with the simulated profile with the best fit shown in figure 7.4(b). The simulated profile arose from a structure with oxygen atoms located in sites directly above the second layer atoms

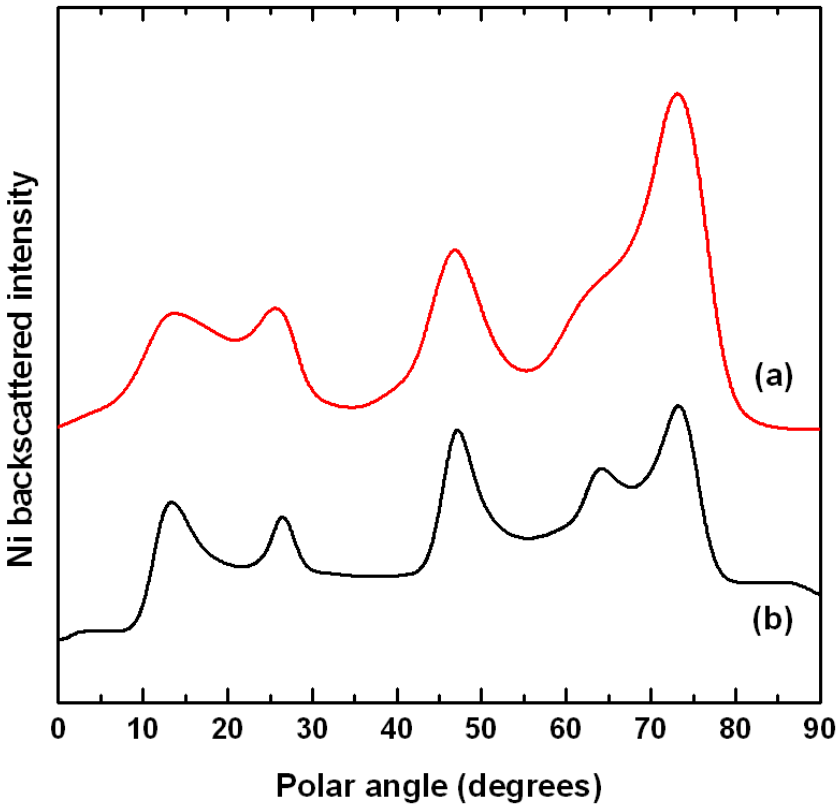

Figure 7.4: (a) Experimental Ni backscattered intensity profile from the Ni(110)-(3×1)-O surface in the <100> azimuth, showing peaks corresponding to scattering from the outermost seven layers of the structure. (b) shows the corresponding profile from the FAN simulation of a trial structure containing expansions in the two outermost interlayer spacings relative to the bulk Ni(110) structure.

at a height of 1.00 Å above the Ni(110) surface layer, with the O atoms occupying every third row in the <100> direction (as previously shown in figure 7.1). This led to an improved fit on the intensity of the surface peak at 14° when compared to the 'missing row' (3×1)-O structure, in which every third row of O atoms is missing, which gave a much-reduced intensity at 14°. The trial structure used to generate the profile shown in figure 7.4(b) contained a $\sim$ 7% expansion of Δ_{12} to 1.33 $\pm$ 0.02 Å. This is in close agreement with the structure found by Favot *et al.* after the adsorption of small amounts of CO on the Ni(110) surface [198], although the expansion is larger than that found by van der Veen *et al.* on the Ni(110)-(3×1)-O surface studied using MEIS [195]. Δ_{23} was found to be 1.30 $\pm$ 0.02 Å, an expansion of $\sim$ 4% on the bulk

value and hence very close to the value obtained from previous studies of the clean Ni(110) surface [12, 197]. Below this, the bulk Ni(110) structure was observed, with interlayer spacings of 1.246 Å. Therefore, the adsorption of just $1/3$ ML of oxygen was found to cause a significant outward relaxation of the surface layer, whilst the structure of the near-surface region was found to be unaffected.

7.4 Pt deposition on the Ni(110)-(3×1)-O surface

To begin this stage of the experiment, 0.30 ± 0.03 ML of Pt was deposited on the Ni(110)-(3×1)-O surface at room temperature. No LEED pattern was observed, indicative of disorder in the surface region caused by the inclusion of Pt atoms. The Pt spectrum extracted from the CAICISS data collected in the <100> azimuth is shown in figure 7.5(a). A brief inspection of this profile shows the existence of features centered at 25°, 47° and 72° arising from the scattering of particles from Pt atoms in the third atomic layer of the structure. This immediately indicates the penetration of Pt atoms into the near-surface region upon sub-monolayer deposition at room temperature, whilst the peak centered at 14° shows a significant amount of Pt in the surface layer. Therefore, on initial inspection, it appears that the adsorption of $\sim$ 0.3 ML of O on the Ni(110) surface prior to Pt deposition is insufficient to prevent Ni-Pt alloy formation in the near-surface region.

Careful analysis of the CAICISS data using the FAN software yielded the Pt backscattered profile shown in figure 7.5(b). In order to replicate the experimental profile, a surface layer with an average Ni_3Pt composition was required, in addition to Pt atoms making up 5% of the second and third atomic layers. The Pt atoms were located at random substitutional sites within the Ni(110) structure in accordance with the disorder indicated by the LEED observations. Interestingly, the analysis of the CAICISS data revealed no discernable change in the atomic structure of the surface region as a result of the inclusion of the Pt atoms, with Δ_{12} remaining at 1.33 ± 0.02 Å and Δ_{23} remaining at 1.30 ± 0.02 Å. No changes were observed in either the structure or composition of the sample at the fourth layer or below, which retained the bulk Ni(110) structure.

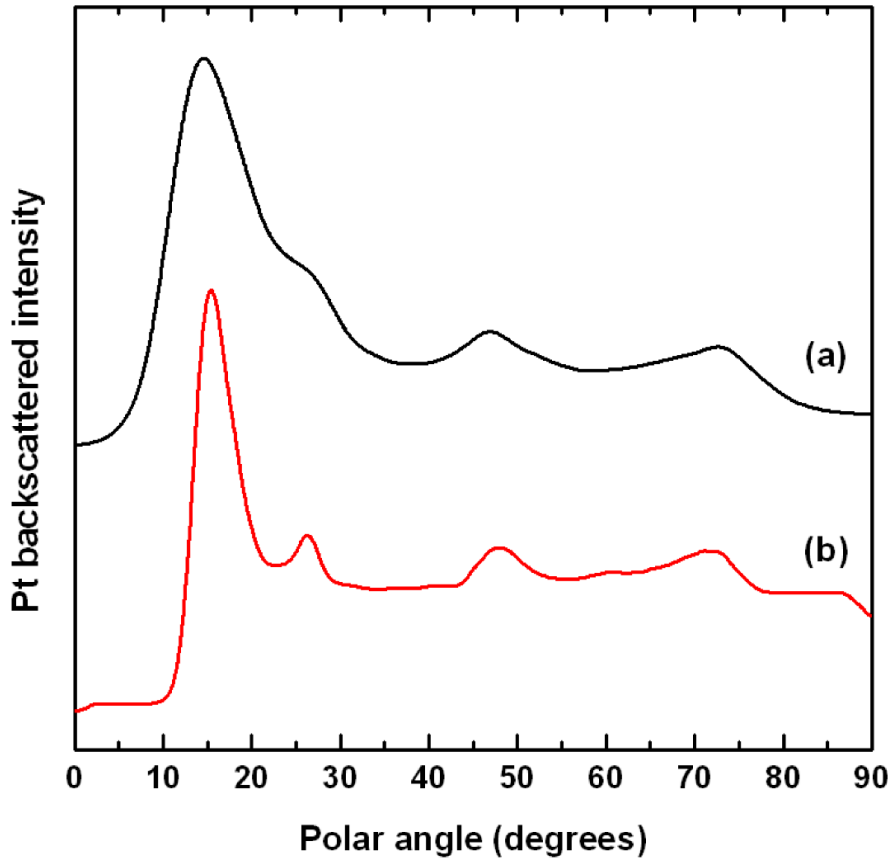

Figure 7.5: (a) The Pt-backscattered intensity profile extracted from the CAICISS data collected in the <100> azimuth following the deposition of 0.30 ML of Pt on the clean Ni(110) surface. (b) The simulated Pt profile giving the best fit of these data. The final structure and compositional profile is summarized in table 7.1.

With the existence of a substitutional alloy at sub-monolayer Pt coverage confirmed, Pt deposition continued up to a total coverage in excess of a monolayer. CAICISS data were taken at coverages of 0.88 $\pm$ 0.04 ML and 1.88 $\pm$ 0.05 ML, with the Pt-backscattered intensity profiles extracted from the data taken in the <100> azimuth shown in figure 7.6 and the results of the compositional and structural analysis shown in table 7.1. No LEED pattern was observed at any of the coverages at which the CAICISS data were recorded, indicating that deposition of Pt on the Ni(110)-(3$\times$1)-O surface at room temperature yields structures with little order at the surface in terms of the positioning of the Pt atoms within the Ni(110) structure.

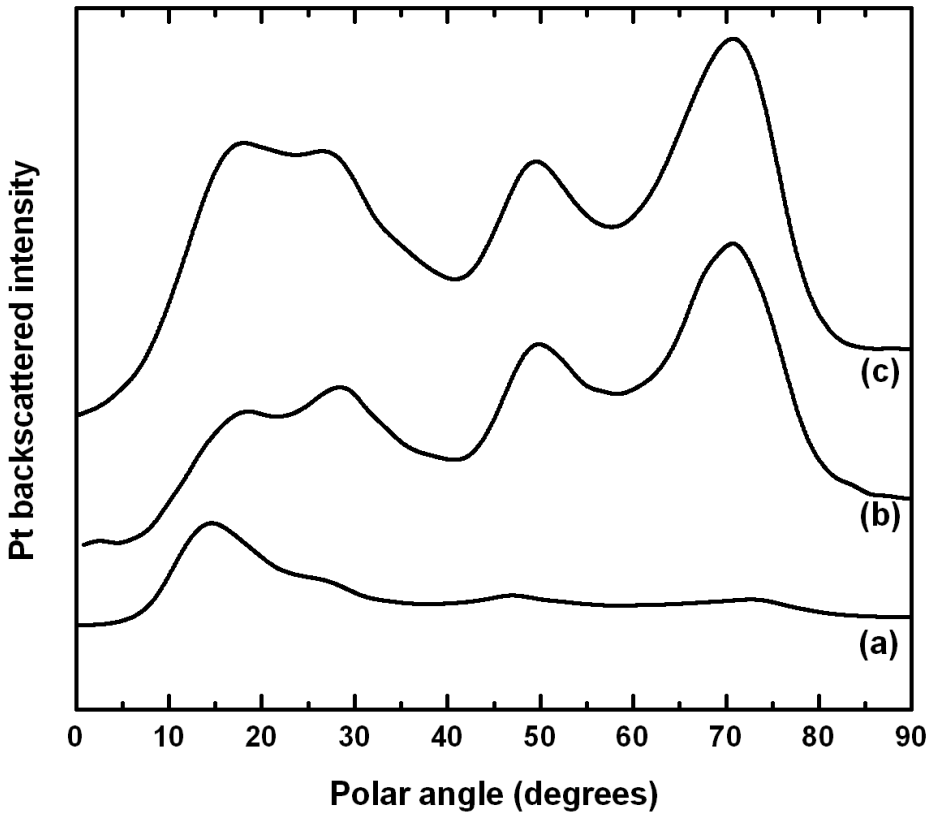

Figure 7.6: The Pt-backscattered profiles extracted from the CAICISS data obtained at Pt coverages of (a) 0.30 ML, (b) 0.88 ML and (c) 1.88 ML on the Ni(110)-(3×1)-O surface. Structural and compositional details are given in the main text and table 7.1.

The Pt-backscattered profiles shown in figure 7.6(b) and (c) show an increasing concentration of Pt atoms in the near-surface region, as evidenced by the increase in intensity of the peaks at polar angles in excess of 20°. Analysis of the profile collected following the deposition of 0.88 ML of Pt using the FAN software revealed the penetration of Pt atoms as far as the fourth atomic layer. The analysis showed that Pt atoms constituted 33 ± 3% of the surface layer, 25 ± 2% of the second layer and 15 ± 2% of both the third and fourth atomic layers.

Due to the lattice mis-match between Ni and Pt of 11.3%, the inclusion of a significant number of Pt atoms into a structure such as Ni(110) typically leads to expansions in the interlayer spacings. This trend is shown by the increase in the polar angle of $\sim 2^{\circ}$ for the peaks which correspond to scattering from sub-surface Pt atoms

Pt coverage (ML)	**0.00**	**0.30**	**0.88**	**1.88**
Surface layer Pt %	–	25	33	60
Layer 2 Pt %	–	5	25	55
Layer 3 Pt %	–	5	15	35
Layer 4 Pt %	–	0	15	20
Layer 5 Pt %	–	0	0	18
(3×1) - surface (Å)	1.0	1.0	1.2	1.3
Δ_{12}	+6.7%	+6.7%	+12.4%	+12.4%
Δ_{23}	+4.3%	+4.3%	+12.4%	+12.4%
Δ_{34}	0	0	+4.3%	+4.3%
Δ_{45}	0	0	0	0

Table 7.1: A summary of changes to the interlayer spacings and layer-by-layer concentrations during the deposition of Pt on the Ni(110)-(3×1)-O surface.

as the Pt coverage increases from 0.30 ML to 0.88 ML. Analysis of the intensity profile shown in figure 7.6(b) using the FAN software showed that Δ_{12} and Δ_{23} had both increased to 1.40 ± 0.02 Å, a ∼ 12% expansion on the bulk Ni(110) interlayer spacing, whilst Δ_{34} had expanded to 1.30 ± 0.02 Å, an expansion of ∼ 4%. In order to accurately fit the shapes of the peaks observed, the (3×1)-O layer had to be moved to a height of 1.20 ± 0.05 Å above the surface layer of the alloy structure, again most probably due to the inclusion of the larger Pt atoms in the surface region.

The next Pt deposition stage, up to a total coverage of 1.88 ML, led to the inclusion of most of the newly-deposited Pt into the two outermost layers of the crystal. The Pt concentration in the surface layer was observed to have increased to 60 ± 3%, whilst the second layer Pt concentration increased to 55 ± 3%. This is evidenced by the increase of the intensity of the surface peak shown in figure 7.6(c) relative to the other peaks in the Pt-backscattered profile when compared to the profile obtained at a Pt coverage of 0.88 ML. The remaining newly-deposited Pt was found to have migrated to the near-surface region, increasing the Pt concentration to 35 ±

2% in the third layer, 20 ± 2% in the fourth layer and 18 ± 2% in the fifth layer. However, the only change observed in the interlayer spacings was a movement of the (3×1)-O layer out to a height of 1.30 ± 0.05 Å above the surface.

To summarise, the deposition of Pt on the Ni(110)-(3×1)-O surface leads to the formation of a Ni-Pt alloy at the surface and in the near-surface region, with the O layer remaining on top of the surface. Significant amounts of Pt were observed in the near surface region at sub-monolayer coverages, with the outermost layers becoming more Pt-rich with continued Pt deposition. The inclusion of Pt into the Ni(110) structure led to increases in the interlayer spacings in the near-surface region, as would be expected due to the large lattice mis-match between Pt and Ni.

7.5 Oxidation of the Ni(110) surface

In the previous section of this chapter, it was determined that Pt deposition on the Ni(110)-(3×1)-O surface led to the formation of a Ni-Pt alloy in the surface region, analogous to the observations of Kellogg following Pt deposition on the clean Ni(110) surface [189]. However, if the chemical and structural properties of the surface are altered prior to Pt deposition (e.g. by oxidation of the Ni(110) surface), it may be possible to grow thin Pt films on top of the surface. The work in this section focusses on the changes to the structure and composition of the Ni(110) surface during oxidation.

7.5.1 LEED observations

The Ni(110) crystal was cleaned once again using the IBA procedure outlined above until a sharp (1×1) LEED pattern was observed at 78 eV, as shown in figure 7.7(a). The surface was then exposed to a series of short O_2 doses, beginning with a 1.0 L exposure which yielded the (3×1)-O added row structure on the surface (figure 7.7(b)). A 1.5 L exposure led to the (2×1)-O layer being formed on the surface, previously shown to correspond to an oxygen coverage of 0.5 ML [193, 199]. A total exposure of 3.0 L led to the formation of the (3×1)-O missing row structure,

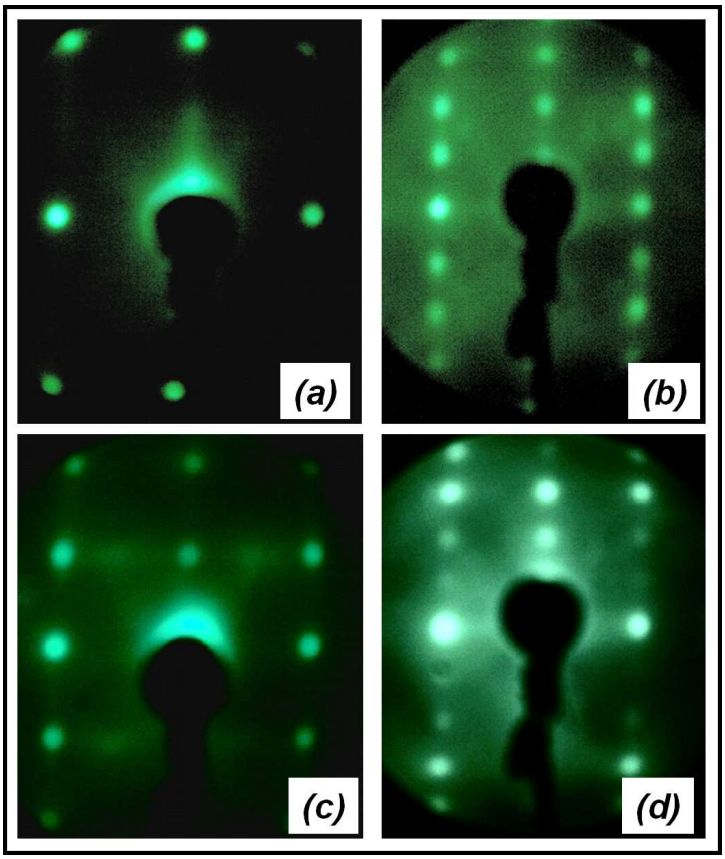

Figure 7.7: (a) The (1×1) LEED pattern recorded from the clean Ni(110) surface, along with (b) the (3×1)-O added row following an oxygen exposure of 1.0 L, (c) the (2×1)-O structure observed following exposure of 1.5 L and (d) the (3×1)-O missing row structure observed following a total exposure of 3.0 L. The clean surface LEED pattern was recorded at 78 eV, whilst the remaining patterns were recorded at 92 eV.

corresponding to a 0.67 ML oxygen coverage. Further exposure of the surface was carried out using atomic oxygen to increase the efficiency of oxidation and led to the increase in the background intensity, obscuring any LEED spots. The (9×5) pattern reported by Eierdal *et al.* was not observed in this investigation [190].

7.5.2 XPS observations

The Ni 2*p* region of the XPS spectra collected following a total atomic oxygen exposure of 1800 L, along with the corresponding region collected from the clean Ni(110) surface is shown in figure 7.8. The clean surface Ni $2p_{1/2}$ and $2p_{3/2}$ peaks

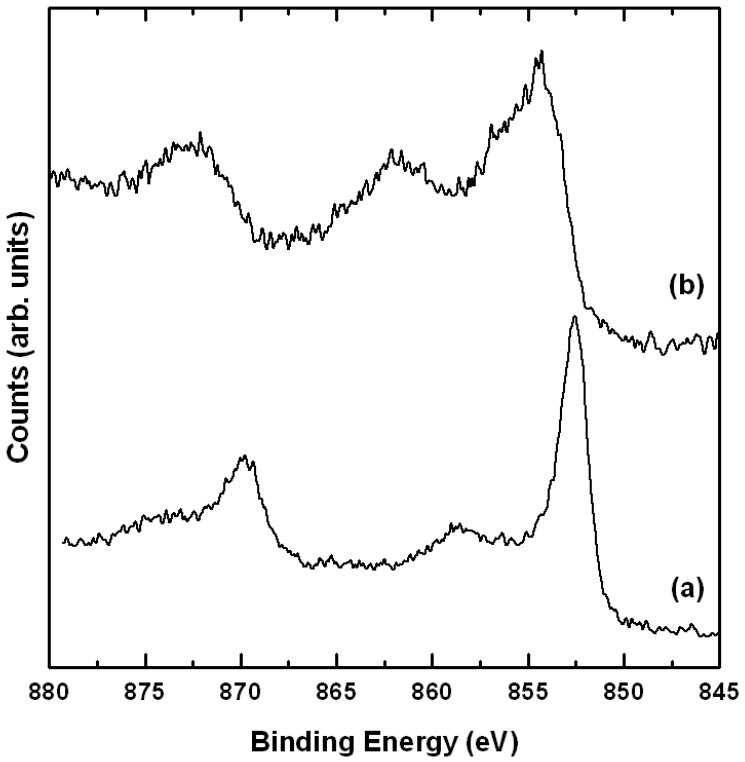

Figure 7.8: The Ni 2*p* regions recorded from (a) the clean Ni(110) surface and (b) following exposure of the surface to 1800 L of atomic oxygen. Significant chemical shifts and no metallic Ni contributions were observed after oxygen exposure, indicating the formation of a thick NiO film.

were observed at 852.5 and 869.8 eV respectively, along with the $2p_{3/2}$ satellite peak at 858.7 eV, and correspond well with previous data from clean Ni surfaces [142]. Chemical shifts in the region of 1.8 eV to 3.2 eV, due to the incorporation of highly electronegative O atoms into the Ni structure, were seen in the XPS data collected following oxidation. Such a spectrum is typical of a nickel oxide surface [142]. No contribution from metallic Ni was observed, suggesting that a reasonably thick NiO film (in excess of 30 Å) had been formed on the Ni surface.

7.5.3 CAICISS investigation of the heavily oxidised surface

Following the exposure of the Ni(110) surface to 1800 L of atomic oxygen, CAICISS data were taken in the <100> azimuth. The Ni backscattered intensity

profile is shown in figure 7.9. The first characteristic to note is that the peak positions arising from the oxidised surface throughout the polar angle range are very similar to those from the Ni(110)-(3×1)-O surface. This observation is in contrast with similar published experiments which have suggested the formation of a NiO(100) film on top of the Ni(110) substrate. This is clearly not the case, as a shift from a (110) surface to a (100) surface would produce large shifts (up to $\sim 8^{\circ}$ in some cases) in the peak positions observed in the CAICISS spectrum due to the different scattering geometries within the f.c.c.(100) structure. Instead, the surface peak appears to have been reduced in intensity as a result of the disorder induced at the surface as a result of oxidation. Beyond that, only small changes to the structure were observed.

Analysis of the Ni-backscattered profile using the FAN software revealed a 6% expansion in both of the two outermost interlayer spacings, Δ_{12} and Δ_{23}. The bulk

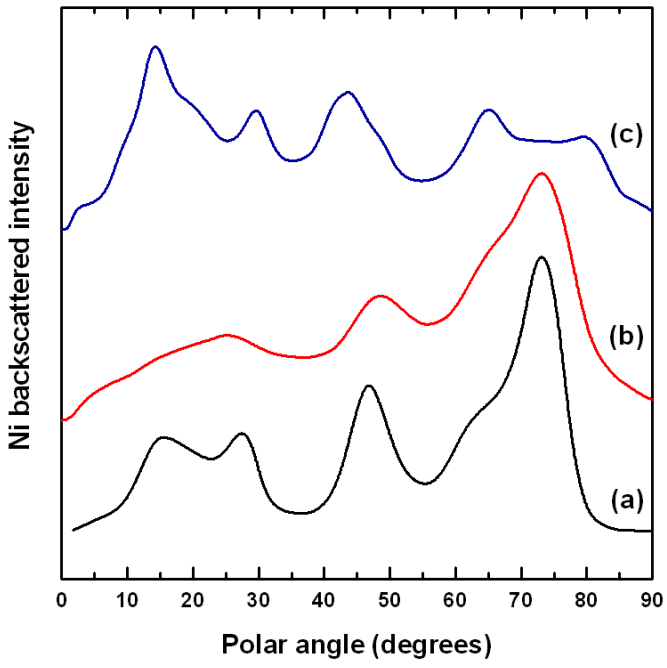

Figure 7.9: The Ni backscattered intensity profiles extracted from CAICISS data recorded from (a) Ni(110)-(3×1)-O surface and (b) the surface following exposure to 1800 L of atomic oxygen. Disorder at the surface is observed by the reduction of the intensity of the surface peak, but the overall structure remains largely unchanged during oxidation. A simulation of a NiO(100) surface (structure taken from [30]) is shown in (c), clearly demonstrating that such a surface has not been formed in this investigation.

Ni(110) structure was observed deeper into the crystal, despite O atoms being found in substitutional sites throughout the probing depth of the CAICISS experiment ($\sim$ 7 layers). Whilst the formation of a thick NiO(110) film leaves the structure of the lattice near the surface practically unchanged when compared to the Ni(110)-(3×1)-O surface, the structure does represent a significant shift away from that of the clean Ni(110) surface [12, 197].

7.6 Pt deposition on the NiO(110) surface

Following the exposure of the Ni(110) surface to 1800 L of atomic oxygen, leading to the formation of a thick NiO(110) film, 0.31 ML of Pt was deposited on the surface at room temperature. The Pt-backscattered intensity profile collected following the deposition is shown in figure 7.10(a). The profile does not exhibit any of the features at polar angles in excess of 25° which correspond to sub-surface Pt atoms as observed following sub-monolayer Pt deposition on the Ni(110)-(3×1)-O surface

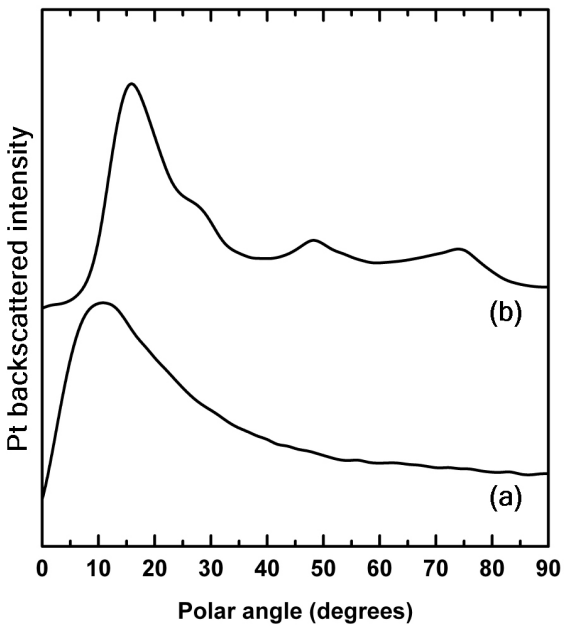

Figure 7.10: (a) The Pt backscattered intensity profile recorded with a 0.31 ML coverage of Pt on the NiO(110) surface. (b) The corresponding data following the deposition of 0.30 ML of Pt on the Ni(110)-(3×1)-O surface, clearly showing a shift in the critical angle and the existence of peaks at higher polar angles associated with the sub-surface Pt atoms.

(figure 7.10(b)). Therefore, virtually all of the Pt atoms must be located in the outermost layer (i.e. on top of the surface). In this case, the surface peak in the Pt profile was observed to have shifted from 16° (Pt on the Ni(110)-(3×1)-O surface) to 10° (Pt on NiO(110)). This indicates a much larger average spacing between Pt atoms in the outermost layer, again a feature which indicates the formation of a Pt overlayer. The surface peak was also broadened in the Pt/NiO(110) case, indicating a range of spacings between Pt atoms on the surface which would only be possible if the Pt atoms were not contained within the NiO(110) structure. No changes were observed in the Ni-backscattered profile (figure 7.11), which would be expected if the relatively large Pt atoms had migrated into the NiO(110) structure.

Further evidence for the formation of a thin Pt layer on top of the NiO film comes from the XPS data recorded following the deposition of Pt on the heavily oxidised

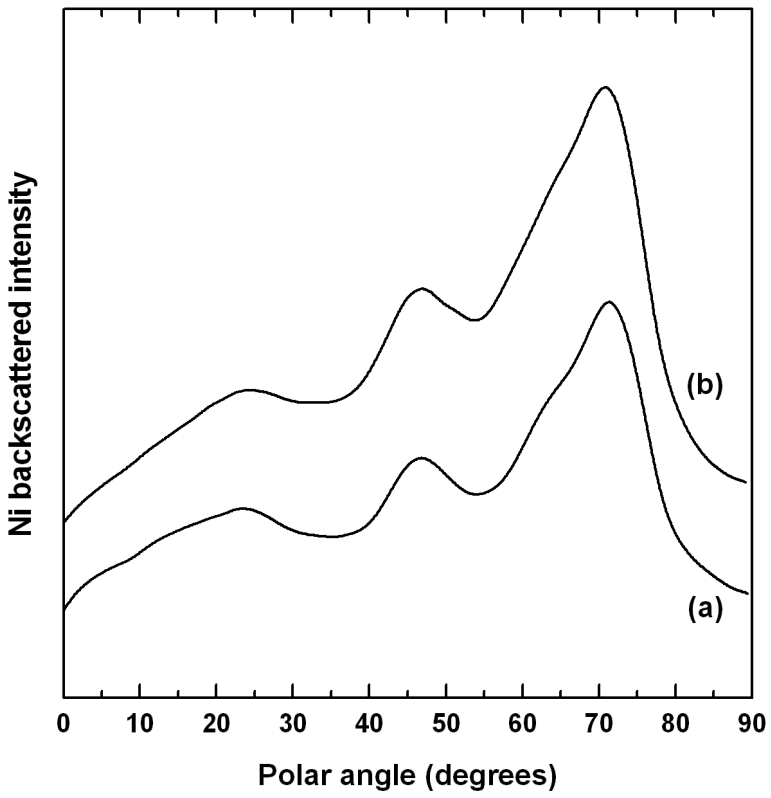

Figure 7.11: The Ni backscattered intensity profiles extracted from the CAICISS data taken (a) prior to and (b) following the deposition of 0.31 ML of Pt on the heavily oxidised Ni(110) surface. No significant changes were observed as a result of the Pt deposition.

Ni(110) surface. The data, presented in figure 7.12 shows a comparison of the Pt $4f$ regions recorded from a clean Pt(111) surface, an oxidised Pt(111) surface and the Pt layer on top of the NiO film. The data collected from both the clean Pt(111) surface and following Pt deposition on the NiO film exhibit just two peaks in the Pt $4f$ region, corresponding to the peaks expected from a clean Pt surface [142]. Data recorded from the Pt $4f$ region following the oxidation of a Pt(111) surface exhibits an additional shoulder at 76.8 eV due to the formation of an oxide layer at the surface. This feature was absent in the Pt $4f$ region recorded following Pt deposition on the NiO film, indicating that there was very little interaction between the Pt and O atoms

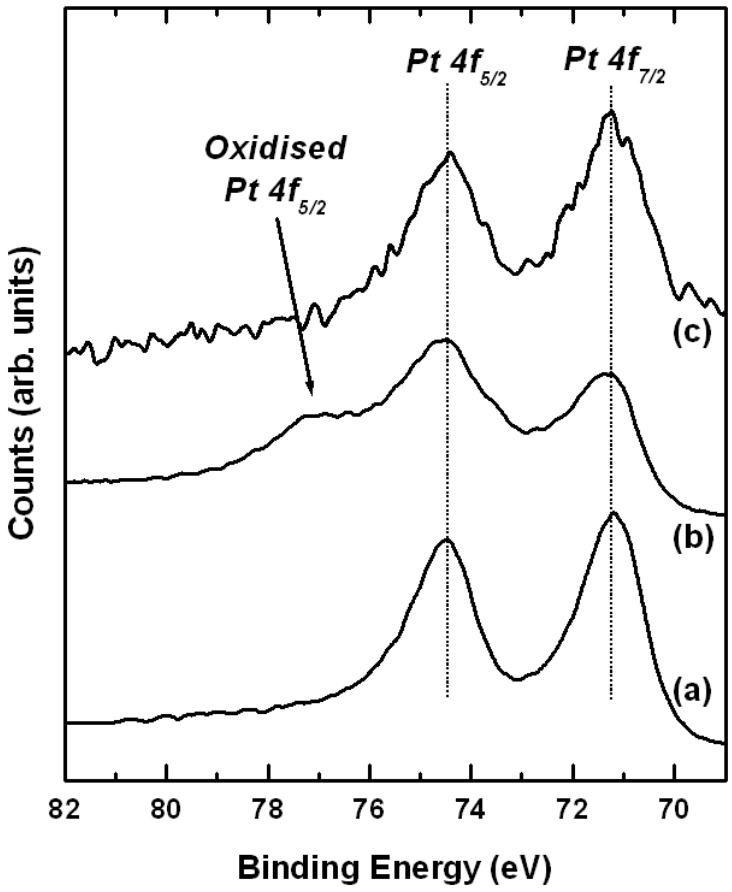

Figure 7.12: The Pt $4f$ region recorded from three different samples. (a) The data recorded from a clean Pt(111) surface. (b) The data collected following the oxidation of the Pt(111) surface (as detailed in chapter 5), showing an additional feature at 76.8 eV. (c) The Pt $4f$ region recorded following the deposition of 0.31 ML of Pt on the Ni(110) surface. Note the shoulder feature at 76.8 eV was not observed in the latter case.

within the sample and pointing to the formation of a Pt overlayer on top of the NiO film.

A second Pt deposition was implemented, bringing the total Pt coverage to 0.80 ML, in order to fully establish the growth mode of Pt on the NiO(110) surface. The Pt-backscattered intensity profile, shown in figure 7.13, again shows a very broad surface peak due to the disorder induced in the NiO(110) structure during the oxidation process. However, no peaks are observed at higher polar angles - peaks which would be present if only a small amount of Pt atoms ($\sim$ 5% of a monolayer) had penetrated into the NiO(110) structure. The surface peak was found to be centered at 17°, a 5° shift to higher angles compared to the data recorded following the 0.31 ML Pt deposition on the NiO(110) surface. This shift should be expected as it arises from the

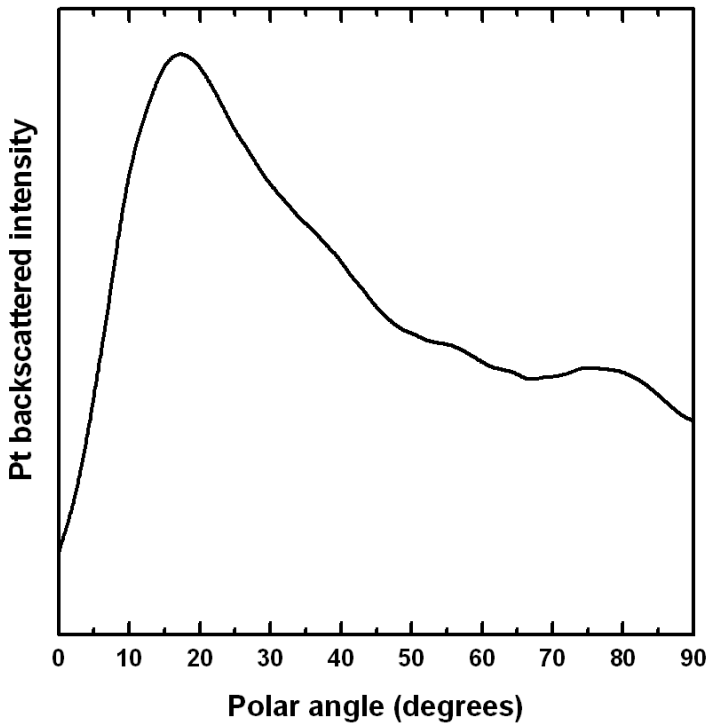

Figure 7.13: The Pt-backscattered intensity profile recorded in the <100> azimuth following the deposition of 0.80 ML of Pt on the NiO(110) surface at room temperature. The broad surface peaks arises from the disorder at the NiO(110) surface prior to Pt deposition, whilst the lack of peaks at polar angles in excess of $\sim$ 30° is indicative of the layer-by-layer growth of a purely Pt film.

shortening of the average spacing between Pt atoms in the <100> direction which occurs as the Pt layer nears completion. All of these observations indicate that a purely Pt film has been formed on top of the NiO(110) surface.

Following the acquisition of CAICISS data at a Pt coverage of 0.80 ML, the sample was annealed to 400°C for 10 minutes. A weak (1×1) LEED pattern was observed on cooling to room temperature, indicating that the surface region had undergone some re-ordering during the annealing. The Pt-backscattered intensity profile extracted from the CAICISS data recorded from this surface is shown in figure 7.14. The surface peak, at 15°, corresponds well with the angle of the surface peak observed following Pt deposition on the Ni(110)-(3×1)-O surface (16°, as shown in figure 7.4). Therefore, it now appears that the Pt atoms are located within the Ni(110) lattice. The peaks centered at 25°, 47°, 63° and 72° all indicate that the Pt atoms

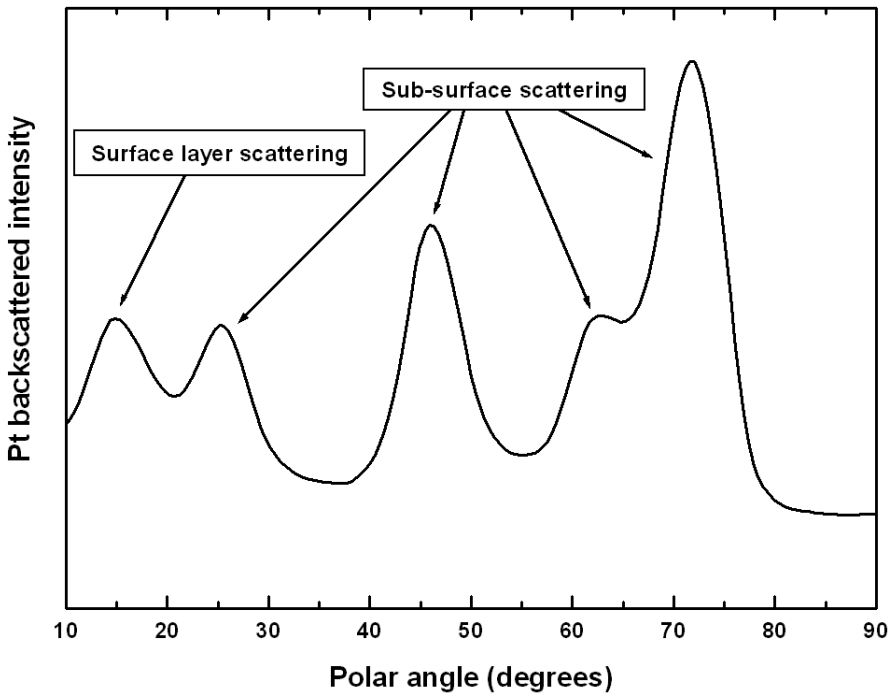

Figure 7.14: The Pt-backscattered intensity profile recorded in the <100> azimuth following annealing of a sample containing a 0.80 ML Pt film on top of a NiO(110) surface to 400°C for 10 minutes. The presence of the sharp peaks at polar angles in excess of $\sim 20^\circ$ indicates a well-ordered structure with a significant amount of Pt atoms which have penetrated into the near-surface region during the annealing process.

have penetrated well below the surface, to at least the fifth layer of the structure. In addition, the annealing appears to have removed a significant proportion of the O atoms and disorder from the surface region, as evidenced by the sharpness of all the peaks in the CAICISS profile. This demonstrates that sub-surface Pt atoms can be clearly observed using CAICISS and that before annealing, the Pt atoms were residing in a purely Pt layer on top of the NiO(110) surface.

7.7 Conclusions

The deposition of Pt on the clean Ni(110) surface has previously been shown to produce a substitutional alloy at the surface [189]. The effect on the growth mode of Pt on Ni(110) surfaces by changing the degree of oxidation to which the surface is exposed has been investigated using CAICISS, LEED and XPS.

Firstly, the surface was exposed to 1.0 L of atomic oxygen, after which LEED indicated that the Ni(110)-(3×1)-O surface had been formed. Analysis of CAICISS data recorded in the <100> azimuth led to the conclusion that this corresponded to the (3×1)-O added row structure, as opposed to the (3×1)-O missing row structure. The CAICISS data also illustrated the relaxations induced in the surface region as a result of the adsorption of just 1/3 ML of oxygen, with the outermost interlayer spacing, Δ_{12}, found to have expanded by $\sim$ 7% with respect to the bulk Ni(110) structure. Δ_{23} was also observed to have expanded to $\sim$ 4% more than the bulk interlayer spacing.

The deposition of 0.30 ML of Pt on the Ni(110)-(3×1)-O surface led to the formation of a Ni-Pt alloy in the surface region. Pt atoms were observed to have penetrated as far as the third layer of the structure, although no changes to the near-surface structure were observed. However, a further Pt deposition which brought the total coverage to 0.88 ML resulted in the first two interlayer spacings expanding to $\sim$ 12% larger than the bulk Ni(110) interlayer spacing, along with a $\sim$ 4% expansion of Δ_{34} due to the inclusion of Pt atoms in the fourth atomic layer. Increasing the deposited Pt coverage to 1.88 ML led to an increase in the Pt concentration in each of the outermost five layers of the structure, but produced no discernable change in

the interlayer spacings in the near-surface region. The (3×1)-O layer was observed to remain on top of the Ni-Pt surface alloy throughout the investigation.

Following the re-preparation of a clean Ni(110) surface, the sample was exposed to a series of short molecular O_2 exposures which allowed the (3×1)-O missing row, (2×1)-O and (3×1)-O added row structures to be observed with LEED. All LEED spots were concealed by the increasing background intensity as the surface was exposed to further amounts of atomic oxygen.

After an extended exposure to atomic oxygen (1800 L), XPS showed that a NiO film of at least 30 Å in thickness had been formed on the surface, with no purely metallic Ni observed within the sampling depth. CAICISS indicated that a NiO(110) film had been produced during the oxygen exposure, contrary to some previous reports which have suggested that this film should take on a NiO(100) structure.

Pt was deposited up to a total coverage of 0.80 ML on the NiO(110) surface at room temperature. CAICISS and XPS observations suggested that all of the Pt atoms were located on top of the NiO(110) surface in a disordered, but purely Pt film, and hence the growth mode of Pt at room temperature was found to be different when compared to the clean Ni(110) and Ni(110)-(3×1)-O surfaces. Annealing of the Pt/NiO(110) structure led to the formation of a Ni-Pt alloy in the near-surface region and the elimination of the Ni-oxide structure.